American Mineralogist, Volume 91, pages 203–210, 2006

A cold-sealing capsule design for synthesis of fluid inclusions and other hydrothermal experiments in a piston-cylinder apparatus

ALISTAIR C. HACK[1,*] AND JOHN A. MAVROGENES[1,2]

[1]Research School of Earth Sciences, The Australian National University, Canberra, ACT 0200, Australia
[2]Department of Earth and Marine Sciences, The Australian National University, Canberra, ACT 0200, Australia

ABSTRACT

Here we report on a newly developed, large-volume, cold-sealed capsule design for hydrothermal synthesis experiments in a piston-cylinder apparatus that should be useful for the production of synthetic fluid inclusions at pressures and temperatures not previously attained in gas- or fluid-pressurized reaction vessels. The design is adapted for large-volume experiments using a 30 mm internal-diameter pressure vessel, but can be scaled down to suit smaller pressure vessels, e.g., 15.9 mm (5/8") internal diameter, if required. Calibration experiments show that temperature varies ±5 °C over the length of a 30 mm (length) × 15 mm (diameter) Cu capsule. The design incorporates the thermocouple within the capsule mass to optimize temperature control. Quartz-hosted H_2O inclusions were synthesized over a range of conditions. Fluid-inclusion densities are consistent with the nominal experimental conditions, suggesting a friction correction is not required. This approach has several advantages over conventional hydrothermal experimental methods: (1) substantially higher pressures are attainable in piston-cylinder than hydrothermal and gas-media apparatus; (2) cold-sealing capsules avoid potential problems associated with welded capsules, such as solution modification; (3) capsule fluids are readily sampled ex situ; (4) the use of relatively thick-walled capsules minimizes H_2-losses during experiments; (5) synthetic fluid inclusions can be used to derive fluid *PVTX* properties by combining conventional thermometry with analyses of individual fluid inclusions or independent mineral solubility data.

Keywords: Piston-cylinder apparatus, synthetic fluid inclusions, hydrothermal studies, fluid *PVTX* properties, high-pressure and -temperature fluids, cold-sealed capsule, isochore

INTRODUCTION

Fluids have been implicated in many geological processes from controlling the location and extent of melting at subduction zones to hydrothermal ore genesis, earthquake generation, and rock-forming processes in general. The quantification of hydrothermal mass fluxes and processes, along with subsolidus and melting phase relations in the upper mantle and crust, requires knowledge of mineral solubilities, chemical speciation, and pressure-volume-temperature (*PVT*) properties of fluids. In principle, the necessary details should be readily obtained by experimentation combined with investigation of natural fluid inclusions, as these contain the sole direct information on natural high-pressure and -temperature fluids. However, our current understanding barely scratches the surface. Simply stated, the paucity of relevant information is due to the limitations of traditional experimental approaches and, until recently, analytical difficulties in extracting detailed chemical information from natural single fluid inclusions. Moreover, deciphering the fluid-inclusion record alone, despite its promise, is not a panacea for an absence of experimental techniques capable of sampling fluids at crustal and upper mantle conditions. For example, fluids entrapped in relatively high *P-T* rocks are scarce and of uncertain origin since they rarely survive exhumation to the surface without modification (Scambelluri et al. 2001). Thus, the rarity and equivocal provenance of fluids encapsulated in natural high-pressure and high-temperature samples means the nature of fluids in these extreme, yet common, environments will remain largely enigmatic without direct experimental investigation.

Experimental synthesis of fluid inclusions provides a means of isolating fluids at high pressure and temperature. This technique relies on the entrapment and preservation of ambient high-temperature fluids as inclusions at growth irregularities that inevitably develop during fracture healing, re-crystallization, and overgrowth of crystal surfaces. Several decades of experiments using hydrothermal- and gas-media apparatus have firmly established the reliability of this technique to sample fluids at high pressure and temperature. On quenching a fluid from high temperatures, solutes commonly precipitate, exsolve, or back-react with coexisting materials. Although the same processes occur within inclusions on quenching, bulk properties (i.e., total composition and molar volume) of the high-temperature fluid at the entrapment conditions are preserved, because inclusions represent isolated, constant volume systems (ignoring inclusion host solubility for the moment). Accordingly, high-temperature fluid information can be obtained ex situ from single inclusions by combining traditional analytical methods (e.g., microthermometry, Raman spectroscopy) with recent microanalytical developments, such as laser-ablation inductively coupled plasma mass spectrometry (LA-ICP-MS; e.g., Günther et al. 1998), proton-induced X-ray emission spectroscopy (PIXE; e.g., Anderson et al. 1989; Heinrich et al. 1992), and synchrotron X-ray

* Present address: Institute for Mineralogy and Petrology, ETH-Zentrum, 8092 Zürich, Switzerland. E-mail: alistair.hack@erdw.ethz.ch

0003-004X/06/0001–203$05.00/DOI: 10.2138/am.2006.1898

fluorescence and absorption spectroscopic techniques (e.g., SXRF, Mavrogenes et al. 1995; XANES/EXAFS, Anderson et al. 1998; Mavrogenes et al. 2002). Significantly, the synthetic fluid-inclusion technique is not restricted to investigations of single-phase, supercritical fluids, but can also be used to trap coexisting, immiscible "vapor" and "liquid" in non-quenchable, subcritical, two-phase fluid systems as well as sample coexisting hydrous silicate melt and aqueous fluid as inclusions (Bodnar et al. 1985; Student and Bodnar 1996). The solubility of complex mineral buffer assemblages can also be studied (Hack and Mavrogenes, in preparation).

Despite the potential of this technique, most previous synthetic inclusion studies have been generally restricted to pressures less than 0.5 GPa, temperatures below 800 °C, and to relatively simple fluid compositions. These apparent limitations are a general reflection of the constraints imposed by conventional hydrothermal- and gas-media apparatus, the standard devices used to undertake these experiments, and those associated with traditional single-inclusion analytical techniques. Therefore, it seems sensible to adapt devices already used extensively in experimental petrology for determining phase equilibria at deep crust and upper mantle conditions to the task of fluid-inclusion synthesis.

Piston-cylinder apparatuses are capable of extending the temperature and pressure range of fluid-inclusion synthesis experiments (Boyd and England 1960), but have seen very limited use in this application (Ballhaus et al. 1994; Brodholt and Wood 1994; Frost and Wood 1997; Shmulovich and Graham 1999; Withers et al. 2000). This situation presumably stems from the general use of small-volume capsules that are prone to failure or crushing of single crystals during the experiment or upon quenching, which may prevent entrapment, or preservation, of abundant, well-formed inclusions. Such factors present a challenge since fluid-inclusion synthesis generally requires a large sample volume to contain fragile single crystals and other charge materials. Also the usual method of sealing capsules by arc welding can be somewhat unreliable, as some volatilization is common, which in addition to unknown mass losses, can result in changes to the bulk composition of the sample.

Therefore, to avoid the inherent difficulties associated with standard piston-cylinder capsule and welding methods, a simple, large-volume, cold-sealed capsule technique was devised that can be used in a piston-cylinder apparatus for synthesis of fluid inclusions and any other large-volume hydrothermal experiments.

Capsule and piston-cylinder cell assembly

Figure 1 shows the cold-seal capsule and assembly design. The capsule is comprised of a thick-walled capsule body, open at one end, and a separate lid. Both parts are fashioned so the capsule can be swaged, to form an effective cold-seal, by applying direct pressure prior to mounting the complete assembly into a piston-cylinder apparatus. By following this procedure the potential problems encountered with welding are mitigated and sample loading procedures simplified compared to standard or "open" capsule methods (e.g., Ayers et al. 1992; Brodholt and Wood 1994). The quality of the cold seal can be examined visually before running the experiment. Capsules constructed from pure Cu, pure Au, and pure Ag have been used successfully. Capsule parts were machined from solid round metal bars. In the case of Au, however, this meant recycling clean Au scrap by melting it into a solid slug, which was subsequently machined into a capsule. Aside from cleaning, no further treatment of the capsule parts (e.g., annealing) was required. We have also successfully used scaled-down versions of this capsule and assembly design in 15.9 mm (5/8") diameter piston-cylinder pressure vessels.

The lid fits closely inside the capsule body where it is supported by a ledge recessed into the inside diameter of the opening. The depth of the ledge is such that, with the lid inserted, a lip extends above the upper outer surface of the lid by about 1.5 mm. This lip is swaged, or crimped down, over the lid, giving the capsule a watertight seal. A hydraulic press is used to operate a simple swaging device to create the seal. Figure 2 illustrates the swage tool and its operation. The swaging device consists of a brass die, to support the capsule, and a piston-like swage tool to roll the lip inward and over the lid to cold seal the capsule. The swage tool has at one end a circular depression with rounded edges, its diameter equal to the outer diameter of the capsule, its depth the same as the lip thickness. It is important that the lid, the supporting ledge, and swaging lip of the capsule are cleaned to ensure a proper seal.

A flat-bottomed pit drilled into the lid houses the thermocouple. This is essential for accurate temperature control on

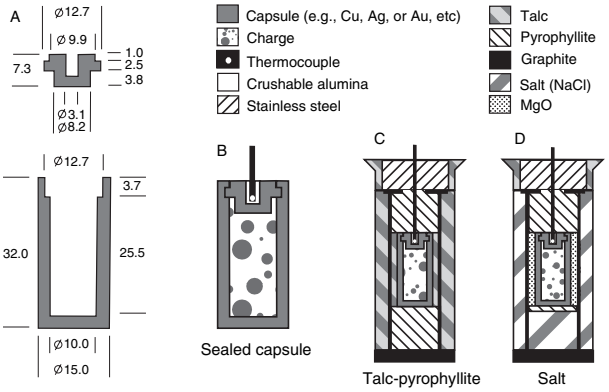

Figure 1. Cold-seal capsule and assembly design for hydrothermal experiments in a piston-cylinder apparatus. (**a**) Cross sectional view of standard capsule body and lid. Dimensions in millimeters (mm). (**b**) Standard capsule. (**c**) Standard talc-pyrophyllite pressure assembly. (**d**) Standard salt pressure assembly.

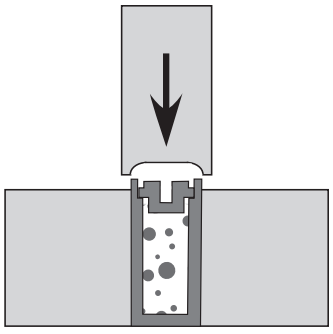

Figure 2. Schematic of swaging device for cold-sealing capsules (cross section).

a capsule of this size. To minimize thermocouple drift due to contamination, the thermocouple and tubing are isolated from the capsule by a crushable alumina sleeve with a small amount of alumina powder packed into the base of the thermocouple recess. The raised portion of the lid prevents collapse of material into the depression, which is otherwise created by the rolled lip that forms the capsule seal and the remaining exposed lid surface. If the space above the lid is not occupied, it collapses during or shortly after pressurization of the cell, which often results in thermocouple failure.

Two pressure-medium configurations, utilizing talc, pyrophyllite, and salt components, were used successfully for hydrothermal and fluid-inclusion experiments (Fig. 1). The talc-pyrophyllite assembly consists of a talc outer sleeve, a graphite heater, and an inner talc sleeve surrounding the capsule. Fire hardened (1050 °C) pyrophyllite spacers were placed above and below the capsule. A graphite disk covers the base of the assembly and a thinner graphite disk was placed at the top of the assembly. The upper and lower graphite disks improve the formation of a reliable heating circuit through the cell.

The salt assembly consists of an outer sleeve of NaCl into which a graphite heater sleeve is inserted. A pyrophyllite (or MgO) sleeve surrounds the capsule, isolating it from the heater. A hardened pyrophyllite spacer sits above, and a thin pyrophyllite disk below the capsule. The thin pyrophyllite disk separates the capsule from an NaCl spacer. Graphite disks are placed at the top and bottom of the cell. All NaCl components were pressed to >95% of the density of crystalline NaCl.

This capsule design, in our experience, is remarkably reliable, capable of remaining sealed at pressures of at least 2.0 GPa, under saline hydrothermal conditions for extended experiment durations, e.g., several weeks (Hack and Mavrogenes, in preparation). Although standard procedures, described elsewhere (e.g., Sterner and Bodnar 1984), can be used for fluid-inclusion synthesis, some points specific to thick-walled capsules in a piston-cylinder are worth mentioning. As with other types of piston-cylinder assembly, pressure is determined from the applied load and can be controlled independently of temperature (i.e., capsules are readily deformed at high pressure and temperature). However, it was found that minimizing the potential volume change (positive or negative) of the capsule during the experiment improved the experimental reliability. A near constant capsule volume is desirable for two reasons: (1) to ensure crystals are not crushed, in the case of fluid-inclusion synthesis; and (2) to reduce the possibility of capsule over-expansion causing fluid loss. This was achieved by calculating the total available sample volume, from the physical dimensions of the capsule body and lid, prior to loading the capsule. After determining the empty capsule volume, the mass of solids and fluids required to produce a bulk capsule isochore equal to or slightly less than that estimated for the conditions of the experiment were calculated. Typically, capsules loaded in this way remain sealed, but are thoroughly annealed after most runs, and show signs of deformation, mostly as minor shortening of the long axis.

Hydrothermal and aqueous fluid- (and silicate melt-) inclusion synthesis experiments in a piston-cylinder apparatus using the capsule and assembly configuration described, can be performed reliably using a "piston-out" routine. Firstly, ~0.2 GPa was applied to the cell prior to heating. Temperature was increased at 50 °C per minute to the desired experimental condition; pressure was added synchronously, such that the *P-T-t* path followed a slightly over-pressured, pure water isochore, appropriate to the desired run *P* and *T*. In general, however, the simple increase in temperature, usually above about 400 °C, saw the cell pressure rise due to the increasing fluid pressure at approximately constant volume. This confirmed that the capsule had sealed, and the assembly approached isochoric behavior on the way to the final experimental conditions. Pressure was adjusted at the final temperature and kept constant for the duration of the experiment by manual adjustment if necessary. Experiments were quenched at 50 °C per minute to avoid thermal shocking of the sample and rupture of fluid inclusions. For the majority of the runs, during the quench process, pressure was decreased by thermal contraction, along the cooling path. However, more controlled quenching along an approximate isochore may be advisable for some conditions to avoid decrepitation or crushing inclusions (e.g., very high-pressure). Temperature ramp rates and temperature during the experiment were controlled automatically via a programmable Eurotherm power controller connected to the thermocouple. The consequence of using relatively low quench rates was not investigated, but for inclusions, it is thought not to affect results because isochore-like *P-T* paths were followed. The advantages of approximately isochoric cooling are: (1) the procedure reduces the chances of inclusion deformation (which would produce erroneous *PVT* fluid inclusion data); and (2) bulk fluid-inclusion composition is not expected to be modified provided the inclusions remained intact during the quench process, which is ensured as far as possible by cooling along an isochore appropriate to the *P-T* conditions.

TEMPERATURE

Several temperature calibration experiments were conducted to determine temperature gradients and the thermocouple position providing the most reliable control. Calibration capsules, constructed from pure copper, were fitted with three thermocouples at different locations within the cell. All calibration experiments were run in standard talc-pyrophyllite assemblies. Rather than use a solid copper capsule, analogue charge materials were placed inside the capsules to simulate normal experimental conditions. Also, to determine whether the charge materials affect the thermal structure of the capsule, two types of analogue charge were used; pyrophyllite, and quartz sand + water. Temperature was measured simultaneously across the capsule, at 10 to 30 °C intervals from 200 to 950 °C using $Pt_{94}Rh_6$-$Pt_{70}Rh_{30}$ (type-B) thermocouples, inserted axially into the assembly. Thermocouples were inside four-bore high-purity Al_2O_3 tubing and surrounded by a slightly larger crushable alumina sleeve to prevent contamination-related thermocouple drift. Pressure was maintained at 500 MPa for calibration of the assembly containing a solid charge. For the hydrothermal charge, an appropriate pure H_2O isochore was followed so as to minimize change in the capsule volume as a function of temperature and thus the failure potential. No correction for pressure was applied to thermocouple EMF measurements.

Experiments containing an analogue charge of quartz sand and water required a special lid to house the thermocouple within

the capsule while retaining a high pressure and temperature fluid phase throughout the calibration experiment. This was achieved using a single-piece flat lid with a hollow spine extending into the capsule, just beyond the center, for thermocouple access (Fig. 3b). On the other hand, a simple flat lid with a hole through it was all that was required for pyrophyllite charge calibration (Fig. 3c). Both lid types were swaged onto the capsules to form the usual cold seal, as described above.

The calibration data show that the temperature profile over the ~30 mm length of the capsule is remarkably uniform, about ±5 °C over the entire temperature range investigated (Figs. 3a and 4). The near constant temperature distribution over the capsule length is attributed to the large mass and high thermal conductivity of copper. In contrast, an extreme thermal gradient, >30 °C/mm, is evident adjacent to the capsule ends, making accurate temperature control difficult to achieve if the thermocouple is placed in the traditional position outside the capsule. Accordingly, our design allows the thermocouple to be embedded within the body of the capsule itself (Fig. 3d).

Figure 4 provides a comparison of temperature measurements made at different positions in copper capsules containing different charge types. The data show that the thermal structure of the capsule is not significantly affected by major differences in experimental charge materials.

PRESSURE

Background

Pressure in a piston-cylinder apparatus is calculated from the applied load, in this case oil pressure, and the effective dimensions of the ram and piston. Typically, the precision of the measurement is about 1–3%.

It is generally believed that pressure uncertainties in a piston-cylinder apparatus largely depend on how well the internal friction-related pressure loss is characterized for the type of assembly used. These so-called "friction losses" are attributed to a variety of sources such as the interaction between the cylinder wall and the piston and, especially, to the effects resulting from the use of cell components with different compressibilities and shear strengths. Although "friction effects" have been calibrated for several salt- and talc-assembly types, "low-friction" and "high-friction" respectively, these calibrations are generally based on short-duration, high-temperature experiments in standard assemblies and are assumed to be independent of temperature, pressure, assembly size, and time (e.g., Green et al. 1966; Boettcher et al. 1981; Bohlen and Boettcher 1982; McDade et al. 2002). However, since large assemblies (30 mm diameter) were used and fluid-inclusion synthesis requires more time than many conventional experiments, the applicability of previous calibrations is uncertain. Moreover, work by Bose and Ganguly (1995) casts doubt on the friction correction concept that pervades the literature. They carefully monitored piston travel, oil pressure and reaction position as a function of time and found that, regardless of assembly type (e.g., talc vs. salt) and assembly size, friction decayed with time, since the reaction position for all assembly types was identical. This observation was taken to imply that pressure corrections become negligible for long (>24 h) duration piston-cylinder experiments. With these considerations in mind, a series of experiments was undertaken to calibrate the pressure loss, if any, due to friction for extended-duration experiments, as typical for fluid inclusion synthesis, in copper capsules within talc-pyrophyllite and NaCl-type assemblies.

Pressure calibration: An application of fluid inclusion synthesis at high pressure

Previous investigations using hydrothermal apparatus have demonstrated that fluid inclusion isochores faithfully record fluid volume as a function of pressure and temperature (Bodnar and Sterner 1985; Sterner and Bodnar 1991; Brodholt and Wood 1994; Frost and Wood 1997; Withers et al. 2000). Here we use synthetic fluid inclusions as a means of calibrating pressure in our piston-cylinder apparatus. The technique depends on accurate knowledge of the experimental T, which was independently calibrated earlier, and the molar volume of water at the experimental conditions. Because the pure water system is univariant everywhere along the vapor-saturation curve, T_h uniquely defines both the homogenization pressure and, importantly, the molar volume of water, which is used for determining the isochore from which the experimental P can be derived. Note, however, isochores should be corrected for the thermal expansivity and compressibility of the host and the amount of quartz dissolved from inclusion walls between T_h and the formation pressure and temperature. These corrections yield the molar volume of the H_2O-SiO_2 fluid mixture ($\overline{V}^{PTX}_{fluid}$) contained within the quartz-hosted inclusion trapped at the experimental conditions. The isochore correction procedure for obtaining $\overline{V}^{PTX}_{fluid}$ is given by Equation 1 (Appendix). Figure 5 illustrates the pressure calibration approach.

Most fluid inclusion PVT studies have been restricted to conditions where the solubility of the host is apparently sufficiently

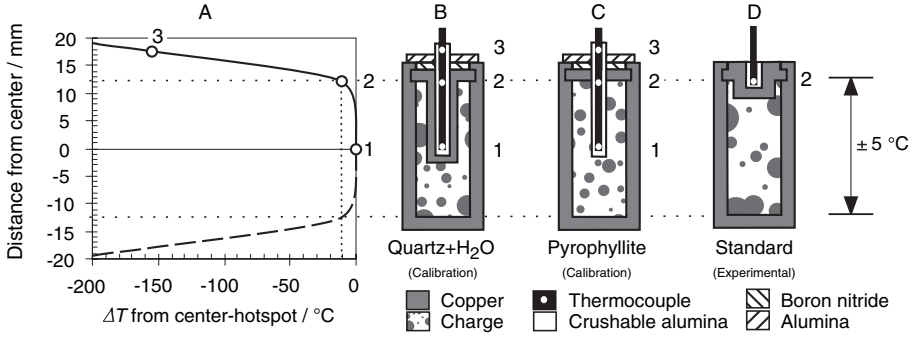

FIGURE 3. (**a**) Temperature gradient measured at 850 °C over 30 mm long copper capsule, in a talc-pyrophyllite assembly. Comparison of modified temperature-calibration capsules containing analogue charges, quartz sand + water (**b**), solid pyrophyllite (**c**), and the standard capsule configuration (**d**). Different thermocouple positions measured (1, 2, and 3).

low to have a negligible effect on the fluid properties. For the quartz-water system this is equivalent to the assumption that the volume of the real fluid ($\overline{V}^{PTX}_{\text{fluid}}$), which does contain dissolved silica is, nonetheless, equal to that of pure H_2O ($\overline{V}^{pure}_{H_2O}$). The validity of this assumption is supported by the data of Bodnar and Sterner (1985) and Sterner and Bodnar (1991), who reliably measured the *PVT* properties of water from 0.1 to 0.6 GPa and 300 to 700 °C using quartz-hosted fluid inclusions. The result was justified on the basis that X_{H2O} is close to unity, as quartz solubility is low at these conditions. However, this assumption is unlikely to be appropriate at higher *P*,*T* conditions where quartz solubilities are known to be much higher, such as near and above the second critical point (i.e., $\overline{V}^{PTX}_{\text{fluid}} \neq \overline{V}^{pure}_{H_2O}$; Kennedy et al. 1962; Nakamura 1974). Such high-solubility conditions are readily accessed with a piston-cylinder apparatus. Furthermore, because the solubility of quartz in H_2O is well known to at least 900 °C and 2.0 GPa (Manning 1994), it is a simple matter to correct an isochore to account for dissolved silica.

Fluid-inclusion synthesis

Capsules were loaded with pure water, pre-cracked quartz, and a small amount of silica powder (about the mass predicted for saturation). Loaded capsules were contained within either NaCl or talc-pyrophyllite assemblies then run at constant pressure and temperature in a piston-cylinder apparatus following the procedure described above. During the experiment, fluid inclusions were formed along annealed fractures.

Fluid-inclusion *PVT* results and discussion

Experimental details and fluid-inclusion data are given in Table 1 and Figure 6. Fluid-inclusion data were combined with volumetric data for quartz (Berman 1988), pure H_2O on the liquid + vapor curve (Haar et al. 1984), and supercritical H_2O (Holland and Powell 1998) to determine $\overline{V}^{PTX}_{\text{fluid}}$ (Eq. 1, Appendix).

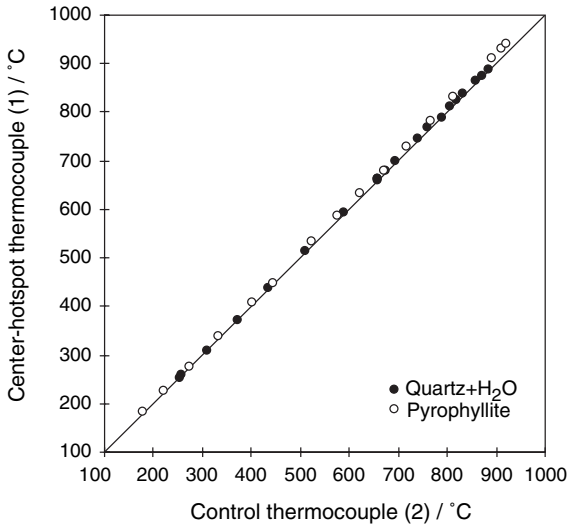

Figure 4. Comparison of temperature-calibration measurements across the copper capsules for pyrophyllite (open symbol) and quartz sand + water (solid symbol) charges. The numbers in parentheses refer to thermocouple positions shown in Figure 3.

There are at least three main sources of error in the measurements, arising from the variation observed in the applied *P* and *T*, and the range of T_h for each sample. However, for completeness, error in the volume properties of the host and error in the fluid composition also contribute to the overall uncertainty and should be included, since the measurements more accurately describe *PVT* relations in the SiO_2-H_2O system. *P* and *T* uncertainties were considered to be equivalent to the total observed variation during the experiment and with an additional ±5 °C added to the uncertainty to account for the measured thermal gradient across the capsule. The *PVT* properties of quartz were assigned an arbitrary 5% error based on the observed differences between various equations of state (EOS; e.g., Hoisieni et al. 1985; Berman 1988; Dorogokupets 1995; Mao et al. 2001). The quartz solubility error is estimated to be 0.020 mol/kg (±1σ, Manning 1994). However, by far the largest and most significant uncertainty relates to the precision of the T_h measurement (Table 1).

A double capsule technique was utilized to investigate whether dissolution of the copper capsule, although minor, might affect the *PVT* properties of the fluid. Practically, this experiment (R168) involved trapping "pure H_2O" fluid inclusions in quartz in a smaller, carbon arc welded, platinum capsule (outside diameter 5 mm, inside diameter 4.6 mm, length ≤20 mm) placed inside a standard copper capsule. The water in the copper capsule provided a hydrostatic *P* environment, transmitting the external *P* through to the flexible inner platinum capsule. Platinum was chosen because it is well tested for synthetic fluid inclusion experiments (e.g., Bodnar and Sterner 1985; Brodholt and Wood 1994).

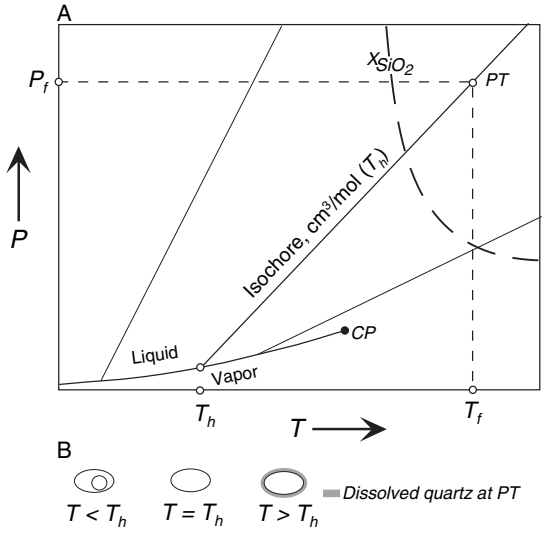

Figure 5. (**a**) Schematic *P*-*T* plot illustrating the pressure calibration approach. H_2O phase relations shown. Straight lines extending from the vapor-saturated liquid curve represent different H_2O isochores. Pressure is determined from T_h and T_f measurements. Abbreviations: T_h is the fluid-inclusion homogenization *T*; T_f, and P_f refer to the fluid-inclusion formation temperature and pressure or actual experimental *P*-*T* condition; *CP* refers the critical point of pure H_2O; X_{SiO_2} refers to mole fraction of SiO_2 dissolved (dashed curve represents a quartz solubility isopleth). (**b**) Schematic illustration of fluid-inclusion behavior during heating from ambient (i.e., $T < T_h$) to the conditions of experimental formation.

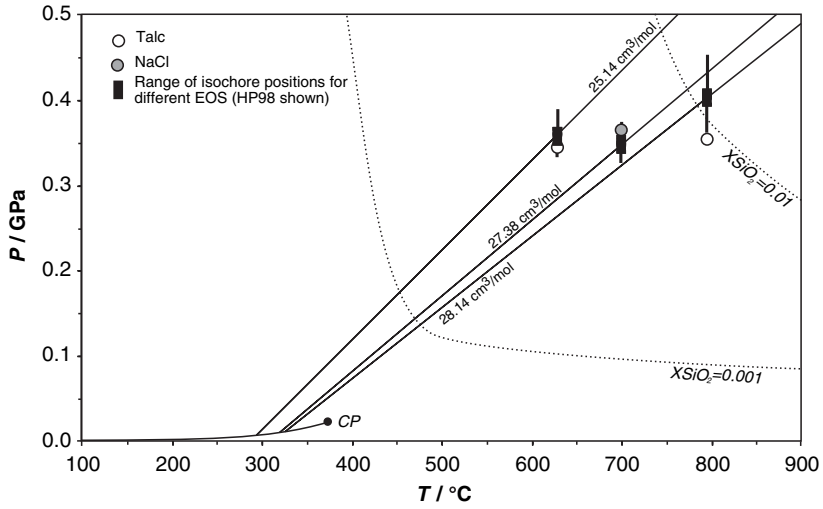

FIGURE 6. *P-T* projection comparing the nominal experimental conditions (circles) with the position of the corrected average isochore determined from the fluid inclusion measurements, $\overline{V}^{PTX}_{\text{fluid}}$. Isochores shown were calculated using the equation of Holland and Powell (1998); error bar reflects the uncertainty in the isochore measurement, whereas the black boxes show the range of discrepancy between different EOS for the same isochore (Burnham et al. 1969; Kerrick and Jacobs 1981; Halbach and Chatterjee 1982; Haar et al. 1984; Saxena and Fei 1987; Holland and Powell 1991, 1998). The piston-cylinder assembly type is also indicated. The quartz solubility as mole-fraction isopleths, 0.001 and 0.01, shown by dotted curves (Manning 1994). The pure water liquid + vapor curve terminates at the critical point, *CP*.

TABLE 1. *PVT* data for quartz-hosted fluid inclusions

Ex.	Assembly	*P*/MPa	*T*/°C	T_h^{ave}	n	σ_{T_h}	$\overline{V}^{T_h}_{min}$	$\overline{V}^{T_h}_{max}$	$\overline{V}^{T_h}_{ave}$	$\overline{V}^{PT}_{fluid}$	$X^{PT}_{SiO_2(aq)}$	$\overline{V}^{PTX}_{fluid}$	$\sigma_{\overline{V}}^{PTX}$
R143	Talc/Cu	354(6)	796(13)	327	13	8.2	26.52	29.20	27.72	27.92	0.0095	28.14	1.33
R166	Talc/Cu	344(3)	629(6)	295	8	1.9	24.74	25.08	24.94	25.05	0.0043	25.14	0.48
R168*	NaCl/Pt	364(6)	700(6)	321	10	2.1	26.08	27.53	27.10	27.23	0.0064	27.38	0.65

Notes: Assembly refers to the piston-cylinder cell type and capsule material used. Numbers in parentheses indicate the uncertainty in the experimental *P* (MPa) and *T* (°C). T_h^{ave} is the average homogenization temperature, and σ_{T_h} is one standard deviation on T_h^{ave}. $\overline{V}^{T_h}_{min}$, $\overline{V}^{T_h}_{max}$, and $\overline{V}^{T_h}_{ave}$ are the minimum, maximum, and average fluid volumes obtained from T_h measurements in units of cm³/mol. $\overline{V}^{PT}_{fluid}$ is $\overline{V}^{T_h}_{ave}$ corrected for the expansivity and compressibility of quartz. $\overline{V}^{PTX}_{fluid}$ is $\overline{V}^{PT}_{fluid}$ further corrected for silica solubility, $X^{PT}_{SiO_2(aq)}$ [specified in mole fraction $SiO_{2\,(aq)}$], as appropriate, and $\sigma_{\overline{V}}^{PTX}$ is the uncertainty in the fluid volume measurement in cm³/mol.
*Indicates double capsule experiment; Pt capsule data reported.

The quartz solubility correction to the fluid volume measurement is minor, particularly in the context of the overall measurement uncertainty. The magnitude of the correction can be evaluated by comparing the composition-corrected fluid volumes, $\overline{V}^{PTX}_{\text{fluid}}$, with the uncorrected volumes, $\overline{V}^{PTX}_{\text{fluid}}$, in Table 1. The compositional correction is minor because quartz solubility is relatively low at the experimental conditions.

In Figure 6 the position of each isochore corresponding to the measured $\overline{V}^{PTX}_{\text{fluid}}$, is plotted in *P-T* space along with the conditions of each experiment. The uncertainty in *P*, related to the precision of the $\overline{V}^{PTX}_{\text{fluid}}$ measurement, is shown at the *T* of the experiment. Uncertainties in $\overline{V}^{pure}_{H_2O}$ arise from the minor variations in *P*, and to a lesser degree *T*, observed during the experiments. There is also some uncertainty in the actual position of the isochores due to the error component attached to the *PVT* properties of pure water, predicted by the EOS. This latter error, however, was ignored, as the same calculations using other EOS yield similar results at these conditions. The extent of discrepancy between alternate EOS (Burnham et al. 1969; Kerrick and Jacobs 1981; Halbach and Chatterjee 1982; Haar et al. 1984; Saxena and Fei 1987; Holland and Powell 1991, 1998) is shown in Figure 6 by the black box through which the isochores of Holland and Powell (1998) project. We avoided conducting isochore-derived pressure calibration experiments at higher pressure, where fluid densities are considerably higher, because this is where isochore *P-T* trajectories between EOS display the most discrepancy (Shen et al. 1993). Moreover, quartz solubility increases with temperature and pressure such that dissolved silica, at more extreme conditions, may have a significant effect on the *PVT* properties of the fluid. Examples of fluid inclusions synthesized at higher pressures will be reported elsewhere (Hack and Mavrogenes, in preparation).

Figure 7 is an alternative presentation of the data, where the measured fluid volume from each sample is compared directly with that of pure water ($\overline{V}^{pure}_{H_2O}$) calculated from the MRK-type EOS given by Holland and Powell (1998) at the same *P* and *T*.

These experiments yield corrected fluid volumes that are indistinguishable from the volume of pure water at the same *P* and *T* given the experimental uncertainties and low concentrations of dissolved SiO_2. *PVT* results from both talc and salt assemblies are similar, suggesting that friction is negligible in both cell types under these conditions.

GENERAL COMMENT

There are several experimental advantages and potential applications arising from the ability to conduct large-volume hydrothermal experiments in the piston-cylinder apparatus. The main advantages include an ability to attain substantially higher pressures than conventional hydrothermal- and gas-media apparatus. The cold-sealing capsule avoids potential problems such as heating, evaporation, and leakage, which are associated with welded capsules. The large capacity of the capsules allows for fluids to be readily sampled ex situ, which can be necessary if compositional information independent of fluid-inclusion analyses is required (e.g., for quantification of inclusion element ratios measured by LA-ICP-MS) or for assessing the extent of fluid modification due to interaction with the capsule or charge materials. In addition to Cu, Au, and Ag also have been used

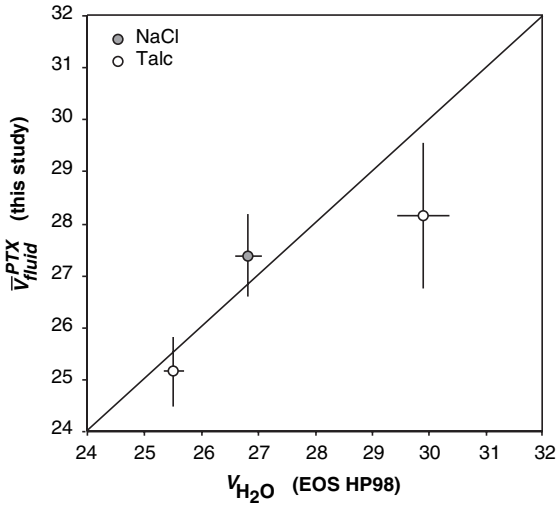

FIGURE 7. Comparison of the measured fluid volume, $\bar{V}^{PTX}_{\text{fluid}}$, and the volume of pure water, V_{H_2O}, at the same P and T calculated using the EOS of Holland and Powell (1998; denoted, HP98). Units are cm^3/mol. The piston-cylinder assembly type used is indicated. Error bars indicate uncertainty in the isochore measurement and the experimental conditions. The uncertainty related to discrepancies between various EOS is not shown (see Fig. 6).

to construct capsules, but other metals and alloys also could be used. For solubility-type experiments in which the capsule participates as a buffering phase (e.g., Loucks and Mavrogenes 1999), the use of alloy capsules would allow metal activities to be varied independently, which would assist in addressing equilibrium and solute speciation issues. Since capsules are relatively thick-walled, H_2 losses during experiments are minimized. Large-volume capsules allow synthesis of large populations of inclusions, which is ideal for production of synthetic inclusion standards, or for the determination of fluid composition by LA-ICP-MS or other techniques that benefit from analysis of multiple individual inclusions from a population. As required, the capsule and cell design can be scaled to fit different piston-cylinder pressure vessel sizes.

The access to high pressures (e.g., 0.2 to ~3.0 GPa) afforded by coupling the cold-sealed assembly with a piston-cylinder device means that synthetic fluid inclusions could be used to determine volumetric properties of mineral-saturated, solute-rich, supercritical fluids, which, unlike fluid compositions, are currently unknown for any "rock"-H_2O system. For example, quartz-hosted synthetic fluid inclusions could be used for measuring the *PVTX* properties of SiO_2-H_2O fluids over a wide range of compositions, such as conditions above the second critical point in the SiO_2-H_2O system (~1080 °C, 1.0 GPa). Above this point, there is no wet solidus; quartz-saturated fluid compositions vary continuously from dilute, H_2O-rich to hydrous silica melt with increasing temperature and pressure (Kennedy et al. 1962; Nakamura 1974; Hack et al., in preparation). This approach could also be extended to other systems, while microanalytical techniques could be used to determine solute speciation and fluid-inclusion compositions.

ACKNOWLEDGMENTS

W. Hibberson, D. Scott, and P. Willis are thanked for invaluable technical assistance and advice. W. Beck-Hansen is thanked for suggesting swaging and for making the swaging tool. H. O'Neill, A. Berry, and J. Hermann are thanked for numerous constructive discussions. Thorough and insightful reviews by G. Morgan and I-M. Chou were appreciated and contributed valuably to the present manuscript. A.C.H. was supported by The Australian National University (Research School of Earth Sciences) through the J.C. Jaeger Scholarship for Ph.D. Research in Earth Sciences.

REFERENCES CITED

Anderson, A.J., Clark, A.H., Ma, X.P., Palmer, G.R., Macarthur, J.D., and Roedder, E. (1989) Proton Induced X-Ray and Gamma-Ray Emission analysis of unopened fluid inclusions. Economic Geology, 84, 924–939.

Anderson, A.J., Mayanovic, R.A., and Bajt, S. (1998) A microbeam XAFS study of aqueous chlorozinc complexing to 430 °C in fluid inclusions from the Knaumuhle granitic pegmatite, Saxonian Granulite Massif, Germany. Canadian Mineralogist, 36, 511–524.

Ayers, J.C., Brenan, J.B., Watson, E.B., Wark, D.A., and Minarik, W.G. (1992) A new capsule technique for hydrothermal experiments using the piston-cylinder apparatus. American Mineralogist, 77, 1080–1086.

Ballhaus, C., Ryan, C.G., Mernagh, T.P., and Green, D.H. (1994) The partitioning of Fe, Ni, Cu, Pt, and Au between sulfide, metal, and fluid phases: A pilot study. Geochimica et Cosmochimica Acta, 58, 811–826.

Berman, R.G. (1988) Internally consistent thermodynamic data for minerals in the system Na_2O-K_2O-CaO-MgO-FeO-Fe_2O_3-Al_2O_3-SiO_2-TiO_2-H_2O-CO_2. Journal of Petrology, 29, 445–522.

Bodnar, R.J. and Sterner, S.M. (1985) Synthetic fluid inclusions in natural quartz, II. Application to PVT studies. Geochimica et Cosmochimica Acta, 49, 1855–1859.

Bodnar, R.J., Burnham, C.W., and Sterner, S.M. (1985) Synthetic fluid inclusions in natural quartz, III. Determination of phase equilibrium properties in the system H_2O-NaCl to 1000 °C and 1500 bars. Geochimica et Cosmochimica Acta, 49, 1861–1873.

Boettcher, A.L., Windom, K.E., Bohlen, S.R., and Luth, R.W. (1981) Low-friction, anhydrous, low-temperature to high-temperature furnace sample assembly for piston-cylinder apparatus. Review of Scientific Instruments, 52, 1903–1904.

Bohlen, S.R. and Boettcher, A.L. (1982) The quartz-coesite transformation: a precise determination and the effects of other components. Journal of Geophysical Research, 87, 7073–7078.

Bose, K. and Ganguly, J. (1995) Quartz-coesite transition revisited: Reversed experimental determination at 500–1200 °C and retrieved thermochemical properties. American Mineralogist, 80, 231–238.

Boyd, F.R. and England, J.L. (1960) Apparatus for phase equilibrium measurements at pressures up to 50 kilobars and temperatures up to 1750 °C. Journal of Geophysical Research, 65, 741–748.

Brodholt, J.P. and Wood, B.J. (1994) Measurements of the PVT properties of water to 25 kbars and 1600 °C. Geochimica et Cosmochimica Acta, 58, 2143–2148.

Burnham, C.W., Holloway, J.R., and Davis, N.F. (1969) Specific volume of water in range 1000 to 8900 bars, 20° to 900 °C. American Journal of Science, 267, 70–95.

Dorogokupets, P.I. (1995) Equation of state for lambda transition in quartz. Journal of Geophysical Research, 100, 8489–8499.

Frost, D.J. and Wood, B.J. (1997) Experimental measurements of the properties of H_2O-CO_2 mixtures at high pressures and temperatures. Geochimica et Cosmochimica Acta, 61, 3301–3309.

Green, T.H., Ringwood, A.E., and Major, A. (1966) Friction effect and pressure calibration in a piston-cylinder apparatus at high pressure and temperature. Journal of Geophysical Research, 71, 3589–3594.

Günther, D., Audétat, A., Frischknecht, R., and Heinrich, C.A. (1998) Quantitative analysis of major, minor and trace elements in fluid inclusions using laser ablation inductively coupled plasma mass spectrometry. Journal of Analytical Atomic Spectrometry, 13, 263–270.

Haar, L., Gallagher, J.S., and Kell, G.S. (1984) Steam tables. Thermodynamic and transport properties and computer programs for vapour and liquid states of water in SI units. Hemisphere Publishing, New York.

Halbach, H. and Chatterjee, N.D. (1982) An empirical Redlich-Kwong-type equation of state for water to 1000 °C and 200 kbar. Contributions to Mineralogy and Petrology, 79, 337–345.

Heinrich, C.A., Ryan, C.G., Mernagh, T.P., and Eadington, P.J. (1992) Segregation of ore metals between magmatic brine and vapor - a fluid inclusion study using PIXE microanalysis. Economic Geology, 87, 1566–1583.

Hoisieni, K.R., Howald, R.A., and Scanlon, M.W. (1985) Thermodynamics of the lambda transition and the equation of state of quartz. American Mineralogist, 70, 782–793.

Holland, T. and Powell, R. (1991) A Compensated-Redlich-Kwong (CORK) equation for volumes and fugacities of CO_2 and H_2O in the range 1 bar to 50 kbar and

100–1600 °C. Contributions to Mineralogy and Petrology, 109, 265–273.
——— (1998) An internally consistent thermodynamic data set for phases of petrological interest. Journal of Metamorphic Geology, 16, 309–343.
Kennedy, G.C., Heard, H.C., Wasserburg, G.J., and Newton, R.C. (1962) The upper three-phase region in the system SiO_2-H_2O. American Journal of Science, 260, 501–521.
Kerrick, D.M. and Jacobs, G.K. (1981) A modified Redlich-Kwong equation for H_2O, CO_2, and H_2O-CO_2 mixtures at elevated pressures and temperatures. American Journal of Science, 281, 735–767.
Loucks, R.R. and Mavrogenes, J.A. (1999) Gold solubility in supercritical hydrothermal brines measured in synthetic fluid inclusions. Science, 284, 2159–2163.
Manning, C.E. (1994) The solubility of quartz in H_2O in the lower crust and upper-mantle. Geochimica et Cosmochimica Acta, 58, 4831–4839.
Mao, H., Sundman, B., Wang, Z., and Saxena, S.K. (2001) Volumetric properties and phase relations of silica - thermodynamic assessment. Journal of Alloys and Compounds, 327, 253–262.
Mavrogenes, J.A., Bodnar, R.J., Anderson, A.J., Bajt, S., Sutton, S.R., and Rivers, M.L. (1995) Assessment of the uncertainties and limitations of quantitative elemental analysis of individual fluid inclusions using synchrotron X-ray fluorescence (SXRF). Geochimica et Cosmochimica Acta, 59, 3987–3995.
Mavrogenes, J.A., Berry, A.J., Newville, M., and Sutton, S.R. (2002) Copper speciation in vapor-phase fluid inclusions from the Mole granite, Australia. American Mineralogist, 87, 1360–1364.
McDade, P., Wood, B.J., Van Westrenen, W., Brooker, R., Gudmundsson, G., Soulard, H., Najorka, J., and Blundy, J. (2002) Pressure corrections for a selection of piston-cylinder cell assemblies. Mineralogical Magazine, 66, 1021–1028.
Nakamura, Y. (1974) The system SiO_2-H_2O-H_2 at 15 kbar. Carnegie Institution of Washington Year Book, 73, 259–263.
Saxena, S.K. and Fei, Y. (1987) Fluids at crustal pressures and temperatures. I. Pure species. Contributions to Mineralogy and Petrology, 95, 370–375.
Scambelluri, M., Bottazzi, P., Trommsdorff, V., Vannucci, R., Hermann, J., Gomez-Pugnaire, M.T., and Vizcaino, V.L.S. (2001) Incompatible element-rich fluids released by antigorite breakdown in deeply subducted mantle. Earth and Planetary Science Letters, 192, 457–470.
Shen, A.H., Bassett, W.A., and Chou, I.M. (1993) The α–β quartz transition at high temperatures and pressures in a diamond-anvil cell by laser interferometry. American Mineralogist, 78, 694–698.
Shmulovich, K.I. and Graham, C.M. (1999) An experimental study of phase equilibria in the system H_2O-CO_2-NaCl at 800 °C and 9 kbar. Contributions to Mineralogy and Petrology, 136, 247–257.
Sterner, S.M. and Bodnar, R.J. (1984) Synthetic fluid inclusions in natural quartz. 1. Compositional types synthesized and applications to experimental geochemistry. Geochimica et Cosmochimica Acta, 48, 2659–2668.
——— (1991) Synthetic fluid inclusions.10. Experimental determination of P-V-T-X properties in the CO_2-H_2O system to 6 kb and 700 °C. American Journal of Science, 291, 1–54.
Student, J.J. and Bodnar, R.J. (1996) Melt inclusion microthermometry: Petrologic constraints from the H_2O-saturated haplogranite system. Petrology, 4, 291–306.
Withers, A.C., Kohn, S.C., Brooker, R.A., and Wood, B.J. (2000) A new method for determining the P-V-T properties of high density H_2O using NMR: Results at 1.4-4.0 GPa and 700-1100 °C. Geochimica et Cosmochimica Acta, 64, 1051–1057.

MANUSCRIPT RECEIVED JANUARY 17, 2005
MANUSCRIPT ACCEPTED MAY 3, 2005
MANUSCRIPT HANDLED BY JILL PASTERIS

APPENDIX: MOLAR VOLUME OF SiO_2-H_2O FLUIDS FROM QUARTZ-HOSTED FLUID INCLUSIONS

The molar volume of a quartz-saturated H_2O fluid differs from that of pure H_2O at any given pressure and temperature due to the presence of dissolved silica in the fluid. H_2O isochores obtained from quartz-hosted fluid inclusions can be corrected to obtain the molar volume of the SiO_2-H_2O fluid mixture at the pressure and temperature of entrapment using the relation

$$\overline{V}^{PTX}_{\text{fluid}} = \left(\overline{V}^{T_h}_{H_2O} + V^{T_h\ \text{precipitated}}_{SiO_{2(aq)}}\right) \cdot \Delta V^{PT}_{Qz} \quad (1)$$

where, $\overline{V}^{PTX}_{\text{fluid}}$ is the molar volume of the H_2O-SiO_2 fluid, in cm^3/mol, $\overline{V}^{T_h}_{H_2O}$ is the molar volume of pure water on the liquid + vapor curve corresponding to the homogenization temperature (T_h). $V^{T_h\ \text{precipitated}}_{SiO_{2(aq)}}$ is the volume increase per mole of water of the inclusion between T_h and the formation pressure and temperature due to quartz dissolution from the walls of the inclusion. $V^{T\text{precipitated}}_{Qz}$ can be calculated from solubility data and the relation, $V^{T_h\ \text{precipitated}}_{SiO_{2(aq)}} = \overline{V}^{T_h}_{Qz} \cdot m^{PT}_{SiO_{2(aq)}} \big/ 55.51$ where $\overline{V}^{T_h}_{Qz}$ is the molar volume of quartz at T_h, $m^{PT}_{SiO_{2(aq)}}$ is the concentration of dissolved silica at pressure and temperature in mol/kg units, and 55.51 represents the number of moles of H_2O in 1000 g of water. ΔV^{PT}_{Qz} is the fractional change in the volume of quartz between T_h and the pressure and temperature of the experiment (also known as the temperature and pressure of formation, T_f, and P_f, respectively). In the SiO_2-H_2O system, quartz solubility on the H_2O liquid + vapor curve is sufficiently low to have negligible effect on T_h (e.g., Bodnar and Sterner 1985).